

Article

Soil Water Dynamics Under Different Land Uses in Loess Hilly Region in China by Stable Isotopic Tracing

Kang Du , Beiying Zhang * and Linjuan Li

School of Geography, Geomatics and Planning, Jiangsu Normal University, No. 101 Shanghai Road, Tongshan New District, Xuzhou 221116, China; dukang@jsnu.edu.cn (K.D.); lilinjuan@jsnu.edu.cn (L.L.)

* Correspondence: zhangbeiying@jsnu.edu.cn; Tel.: +86-159-5218-3672

Abstract: Exploring soil water dynamics under different land use types is important for water resource management and vegetation restoration in the Loess Plateau. In this study, we investigated the hydrogen and oxygen isotopic compositions of soil water from four different land use types to explore the mechanism of soil water movement and transformation and analyse the influence of land use. The results show that the range of stable isotopes (δD and $\delta^{18}O$) in soil water was smaller than that in precipitation. Values for δD and $\delta^{18}O$ in soil water showed relatively similar temporal variation, heavy isotopes were enriched in the soil water in July and depleted in October. Stable isotope values in shallow (<100 cm depth) soil water and deep (>200 cm depth) soil water were low. The δD and $\delta^{18}O$ values in woodlands decreased gradually with increasing depth. Across the four land use types, the maximum variation in δD and $\delta^{18}O$ was in the shallow depth of the soil profile. Groundwater was recharged mainly from precipitation and then from soil water. The ratio of groundwater recharge by soil water under different land use types followed this rank order: woodland (35.70%) > grassland (31.14%) > shrubland (29.47%) > cropland (29.18%). Matrix flow and preferential flow coexisted during infiltration, and the occurrence of preferential flow was related to the land use type. The main reason for the variation in isotopic composition in soil water is the difference in soil evaporation, which is influenced by different vegetation cover. Owing to the difference in soil evaporation and fractionation, precipitation on cropland, shrubland, and grassland can recharge more soil water than on woodland.



Citation: Du, K.; Zhang, B.; Li, L. Soil Water Dynamics Under Different Land Uses in Loess Hilly Region in China by Stable Isotopic Tracing. *Water* **2021**, *13*, 242. <https://doi.org/10.3390/w13020242>

Received: 17 December 2020

Accepted: 14 January 2021

Published: 19 January 2021

Publisher's Note: MDPI stays neutral with regard to jurisdictional claims in published maps and institutional affiliations.



Copyright: © 2021 by the authors. Licensee MDPI, Basel, Switzerland. This article is an open access article distributed under the terms and conditions of the Creative Commons Attribution (CC BY) license (<https://creativecommons.org/licenses/by/4.0/>).

1. Introduction

Soil water is an important component of terrestrial water resources, particularly in arid and semi-arid regions [1]. Soil water originates only from precipitation in most loess hilly areas, where no irrigation is used. In addition, precipitation and soil water can recharge groundwater through matrix flow and preferential flow [2,3]. In loess hilly regions, precipitation and soil water are vital for agriculture and forestry [4]. Over the past 20 years, the vegetation types on the Loess Plateau of China have changed significantly, which affects the process of soil moisture variation [5–7]. Thus, understanding the mechanism of soil water movement has essential implications for the analysis of groundwater recharge, particularly in loess hilly regions where water resources are in short supply [8].

Stable isotope tracing is an effective method to study soil water movement [9–12]. Zimmermann et al. applied hydrogen and oxygen stable isotope technology to study the movement mechanism of soil water in an unsaturated layer. They reported the isotopic index profile distribution caused by soil evaporation [13]. Thereon, many indoor soil column experiments and field experiments have observed the phenomenon of δD and $\delta^{18}O$ enrichment close to the soil surface and have provided theoretical explanations for it [14,15]. The distribution characteristics of stable isotopes in soil profiles are widely used to explore the groundwater recharge mechanism [16–20]. Stable isotopes have been widely

employed to analyse the relationship between soil water and vegetation [21–23]. Using stable isotope data from soil and plant xylem samples from the Scottish Highlands, Geris et al. provided preliminary insights into the spatial pattern and temporal dynamics of soil–plant water interactions [24]. Gao et al. used stable isotopes to study soil moisture in active layers under different land cover types in the Qinghai–Tibet Plateau, indicating that preferential flow often occurs in the degraded alpine meadows, which provide deeper water supply to the groundwater [25]. Song et al. studied the water use patterns of non-native and native woody species in semi-arid sandy land in Northeast China by using stable isotopes, indicating that native woody species mainly used soil water, whereas non-native species depended on groundwater, particularly under low soil water content conditions [26]. Understanding the soil water movement process under different land use types is of great significance for water resource management and plant utilisation of water resources [27,28]. In research on soil moisture in the Loess Plateau of China, many studies have been conducted using stable isotopes in combination with ecological restoration [29–31]. These studies have laid a foundation for the study of soil water using hydrogen and oxygen stable isotope tracers in the Loess Plateau area, while the study of soil water dynamics and groundwater recharge under different land use types still needs to be further investigated.

In this study, we selected four typical land uses and determined their soil water content and stable isotopes in soil water, precipitation and groundwater, to explore the mechanism of soil water movement and analyse the influence of land use type on soil water dynamics.

2. Materials and Methods

2.1. Study Area

The study area is the mountain testing ground of the Ansai Agricultural Ecology Experimental Station ($36^{\circ}51'30''$ N, $109^{\circ}19'23''$ E) of the Chinese Academy of Sciences (Figure 1). It is located in Ansai County, Yanan City, Shaanxi Province, in the hinterland of the Loess Plateau. Its geomorphic type is a typical loess hilly region, and it is situated between 1068 m and 1309 m. The climate of the study area is semi-humid to semi-arid with dry windy springs, hot and rainy summers, and dry cold winters. The annual average temperature is 8.8°C , and the frost-free period is approximately 143–174 days. The average annual precipitation in this area is 500 mm, which mainly occurs between July and September. The vegetation type of the study area belongs to the forest steppe area, with the transition from deciduous broad-leaved forest to steppe in the warm temperate zone, which is also a typical area with affected by soil and water loss due to human activities. The common types of land use are cropland, grassland, shrubland, and woodland. Woodland, shrubland, and grassland species are locust (*Robinia pseudoacacia*), sea buckthorn (*Hippophae rhamnoides*), and purple alfalfa (*Medicago sativa*), while the crops are mainly millet (*Setaria italica*) and corn (*Zea mays*). The soil type is the interlaced area of loessal soil and sand loess.

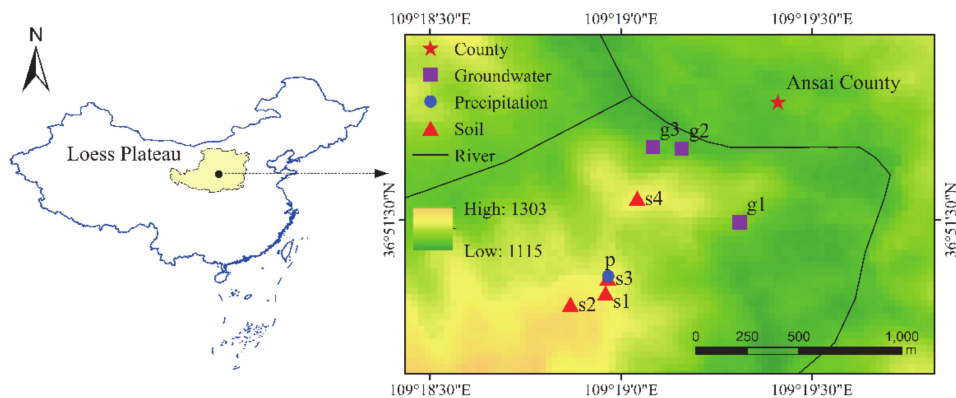


Figure 1. Location of the study area and the sampling sites: Precipitation (p), Groundwater (g₁, g₂, g₃) and soil (s₁, cropland; s₂, grassland; s₃, shrubland; s₄, woodland)

2.2. Sampling Methods

Soil samples were taken with a soil borer at 10 cm depth intervals at depths of 0–100 cm and at 20 cm depth intervals at depths of 100–300 cm at every study site in July, August, and October, 2019. Then, the aluminium boxes containing the soil samples were brought back to the laboratory, and the gravimetric water content of each soil sample was determined by oven-drying. Four soil samples 0–30 cm, 80–100 cm, 180–200 cm, and 280–300 cm were taken and stored frozen at -20°C for isotopic analysis. Meanwhile, ten precipitation samples and forty groundwater samples were collected. The distance between sampling sites was less than 1000 m and, therefore, we considered that all sampling sites were subjected to the same precipitation regime and received the same rainfall amount. Precipitation was collected from rain gauges placed on the flat ground near the shrubland study site. Groundwater samples were also collected from nearby springs located on the half up hills. Polyethylene plastic bottles (100 mL) were used to collect water samples. During collection, the sampling bottle was first rinsed three times with raw water which is the same as the water sampled later, and then filled with water samples. Then, the sealed sampling bottle was refrigerated at 4°C before stable isotope analysis [32].

2.3. Gravimetric Water Content

The total weights of soil samples were determined using a high-precision balance. Then, the dry soil weight was determined by drying soil samples at 105°C for 12 h.

$$\text{SWC}(\%) = (M - M_S)/M_S \times 100 \quad (1)$$

where SWC is the soil water content, M is the wet soil weight (g), and M_S is the dry soil weight (g).

2.4. Stable Isotopic Composition Measurements

Soil water was extracted using a LI-2000 vacuum extraction system (LICA, HongKong, China). The δD and $\delta^{18}\text{O}$ values of all water samples were quantified using a liquid water isotope analyser (IWA-45EP, Los Gatos Research Inc., MA, USA) at the State Key Laboratory of Soil Erosion and Dryland Farming on the Loess Plateau, Institute of Soil and Water Conservation Chinese Academy of Sciences with measurement accuracies of $\pm 1\text{‰}$ and 0.2‰ , respectively. Results were expressed as δ values (‰) with reference to Vienna Standard Mean Ocean Water (VSMOW), as follows:

$$\delta(\text{‰}) = \left(\frac{R_{\text{sample}} - R_{\text{vsmow}}}{R_{\text{vsmow}}} \right) \times 1000 \quad (2)$$

where R_{sample} is the D/H atoms or $^{18}\text{O}/^{16}\text{O}$ ratio in the water sample, and R_{vsmow} is the D/H atoms or $^{18}\text{O}/^{16}\text{O}$ ratio of the VSMOW sample.

2.5. Calculation of Water Supply Ratio

According to the law of isotope mass conservation, by comparing different water isotopes, an end member mixture model can be applied to determine the proportions of water supply between precipitation, soil water, and groundwater [33–35]. The precipitation and soil water is the supply source and groundwater is the mixed pool, the linear algebraic equation is as follows:

$$C(V_A + V_B) = AV_A + BV_B \quad (3)$$

$$C = A \frac{V_A}{V_A + V_B} + B \frac{V_B}{V_A + V_B} = A(1 - x) + Bx \quad (4)$$

where A , B , and C are the precipitation, soil water, and groundwater stable isotope values (‰), respectively; V_A is the amount of precipitation; V_B is the amount of soil water; x is the recharge proportion of soil water; and $(1 - x)$ is the recharge proportion of precipitation.

2.6. Statistical Analysis

Statistical analysis was completed using OriginPro9.0 (OriginLab, Northampton, MA, USA) and SPSS19.0 (IBM, Beijing, China). One-way ANOVA followed by the Tukey's HSD test ($p < 0.05$) was used for evaluating the effect of the month, soil depth and vegetation on the hydrogen and oxygen isotopes in soil water. The study area map was drawn using ArcGIS 10.2.

3. Results

3.1. Stable Isotopic Composition of Soil Water in Different Land Use Types

The isotopic composition of soil water in the study area ranged from -39.34‰ to -77.31‰ (δD) and -3.19‰ to -10.52‰ ($\delta^{18}\text{O}$), the isotopic composition of precipitation ranged from -22.65‰ to -94.76‰ (δD) and -5.98‰ to -14.84‰ ($\delta^{18}\text{O}$), the isotopic composition of groundwater ranged from -32.79‰ to -61.48‰ (δD) and -4.84‰ to -9.60‰ ($\delta^{18}\text{O}$) (Table 1). The range of stable isotopes (δD and $\delta^{18}\text{O}$) in soil water was smaller than that of precipitation. Due to the fact that water vapor source of precipitation is more complex than that of soil water and groundwater, the standard deviation of δD and $\delta^{18}\text{O}$ in precipitation is larger at 20.45‰ and 2.59‰ , respectively. Groundwater is more stable, with standard deviations of δD and $\delta^{18}\text{O}$ of 6.32‰ and 1.13‰ , respectively.

Table 1. Stable isotopic composition of soil water from four different land uses, precipitation, and groundwater.

| Sites | δD (‰) | | | | $\delta^{18}\text{O}$ (‰) | | | |
|---------------|----------------|--------|--------|----------|---------------------------|--------|-------|----------|
| | Max | Min | Mean | St. Dev. | Max | Min | Mean | St. Dev. |
| Cropland | -42.46 | -73.57 | -54.82 | 8.73 | -4.07 | -9.94 | -6.49 | 1.68 |
| Grassland | -39.34 | -76.34 | -56.62 | 9.27 | -4.05 | -10.52 | -6.66 | 1.78 |
| Shrubland | -40.66 | -77.31 | -55.67 | 10.68 | -3.19 | -10.10 | -6.52 | 2.08 |
| Woodland | -39.69 | -70.77 | -54.50 | 9.63 | -3.81 | -9.68 | -6.99 | 2.03 |
| Precipitation | -22.65 | -94.76 | -50.75 | 20.45 | -5.98 | -14.84 | -9.24 | 2.59 |
| Groundwater | -32.79 | -61.48 | -54.10 | 6.32 | -4.84 | -9.60 | -8.44 | 1.13 |

The stable isotopes (δD and $\delta^{18}\text{O}$) of soil water clearly decreased ($p < 0.05$) over time (Figure 2); the variation of δD and $\delta^{18}\text{O}$ under four land uses followed this rank order: July > August > October. Heavy isotopes were enriched in the soil water in July and depleted in October.

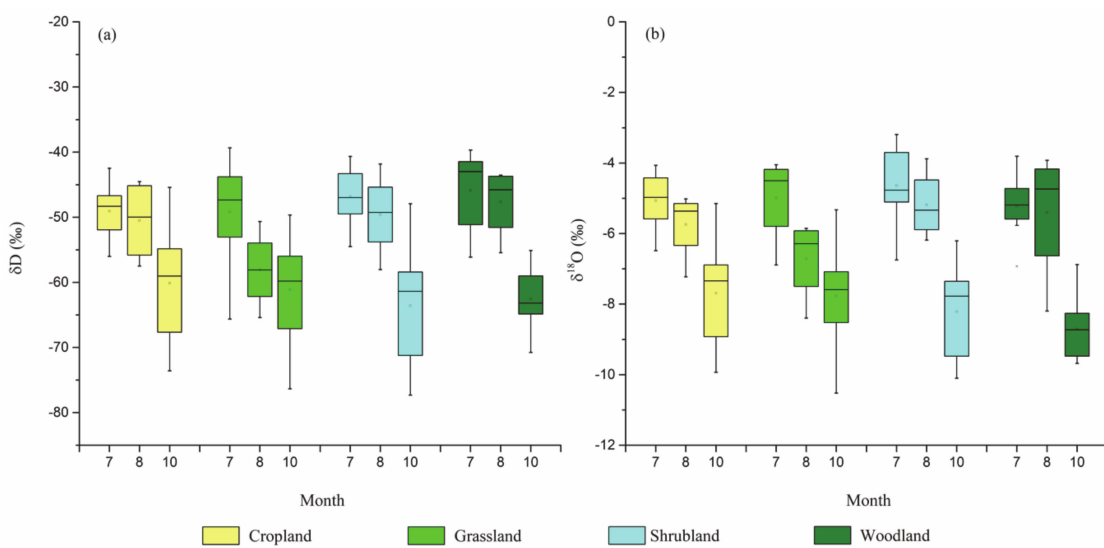


Figure 2. Temporal variations in δD and $\delta^{18}O$ in soil water under four land uses over the current study ((a) δD , (b) $\delta^{18}O$).

3.2. Vertical Distribution Characteristics of Stable Isotopes in Soil Water

The maximum variation in hydrogen and oxygen stable isotopes was observed in the shallow layer (0–100 cm depth) (Figure 3). The deepest level (200–300 cm depth), showed the smallest variation in cropland and woodland whereas the smallest variation observed in grassland and shrubland was in the middle layer (100–200 cm depth). In addition, the variation in soil water content at 0–100 cm depth was larger than that at 100–300 cm depth under the four land uses (Figure 4). Precipitation has a significant influence on the soil water content and stable isotope composition of hydrogen and oxygen in the shallow layer, and the soil moisture, D, and ^{18}O , fluctuated significantly [36]. The vertical distributions of δD and $\delta^{18}O$ in soil water were similar (Figure 5). The maximum value of δD and $\delta^{18}O$ in cropland and grassland was found at 100 cm depth, whereas the maximum value in shrubland was found at 200 cm depth. δD and $\delta^{18}O$ in woodland decreased gradually with increasing depth overall, and the $\delta^{18}O$ value tended to increase below 200 cm depth, due to water mixing changes δD and $\delta^{18}O$ in soil water. The content of soil moisture under four land uses was largest in the shallow layer (0–100 cm depth), and the inflection point of soil water content appeared at a depth of 100 cm. The water content of woodlands below the 100 cm depth was stable at approximately 5%, which indicated that the locust root distribution was deeper than in other vegetation types, and the soil water absorbed by the root caused the soil water profile to be persistently at low values.

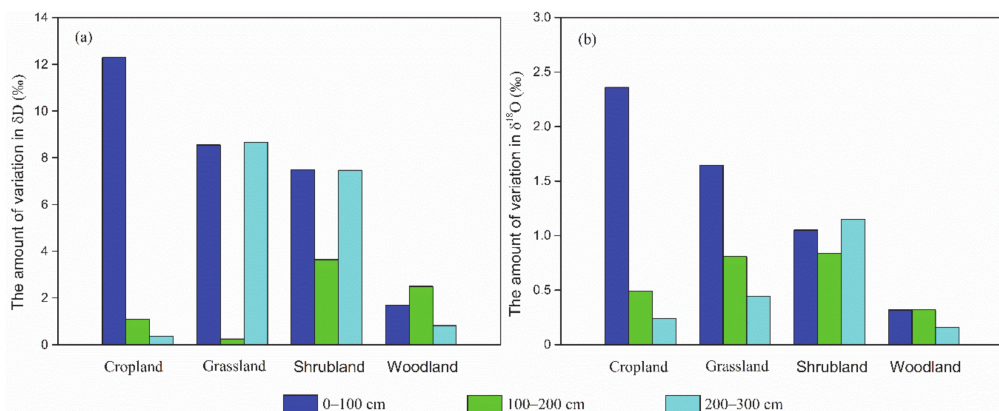


Figure 3. The amount of variation in δD and $\delta^{18}O$ in different soil layers under the four land uses considered in the current study ((a) δD , (b) $\delta^{18}O$).

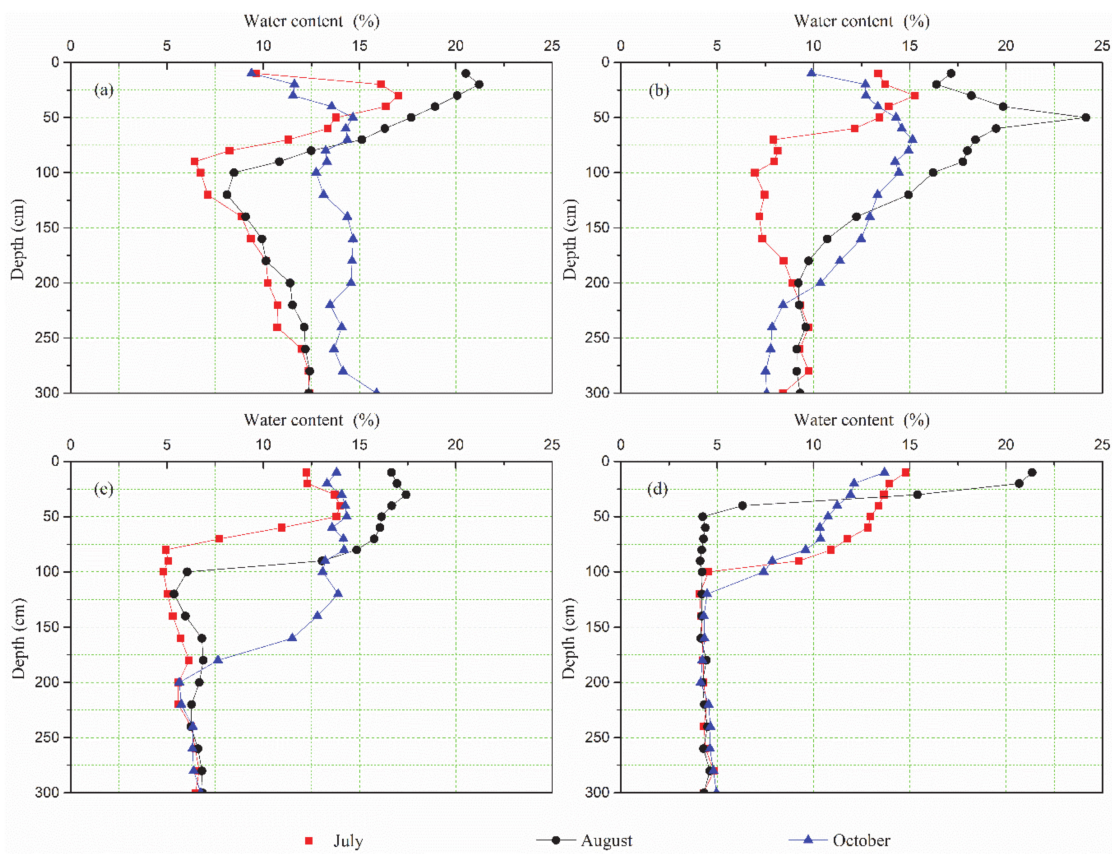


Figure 4. Profile distributions of soil water content under different land use types ((a) cropland, (b) grassland, (c) shrubland, (d) woodland).

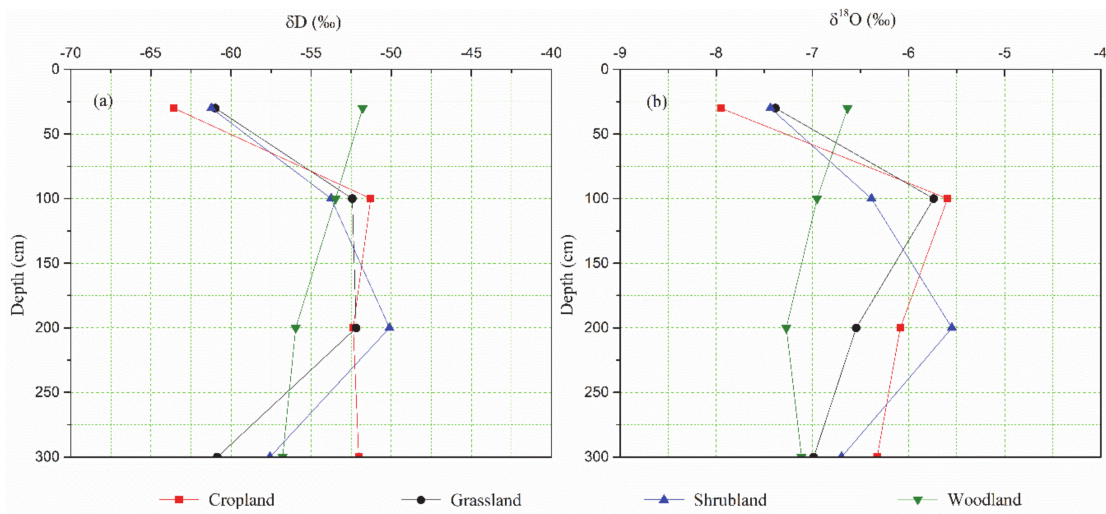


Figure 5. Profile distributions of δD and $\delta^{18}O$ in soil water under different land use types ((a) δD , (b) $\delta^{18}O$, measurements date: 17 June 2020).

3.3. Relationship between Recharge and Transformation of Different Water Bodies

Table 2 shows the proportion of groundwater recharge by precipitation and soil water. Soil water recharged by precipitation consequently transformed into groundwater under certain land use. The proportion of groundwater recharge by precipitation and soil water was 70.82% and 29.18% in the cropland, 68.86% and 31.14% in the grassland,

70.53% and 29.47% in the shrubland, and 64.30% and 35.70% in the woodland, respectively. The proportion of groundwater recharge by soil water under the four land use types follows this rank order woodland > grassland > shrubland > farmland, and precipitation was the main recharge source of groundwater.

Table 2. Estimation of groundwater recharge ratio by soil water and precipitation under different land uses.

| Sites | $\delta^{18}\text{O}$ (‰) | | | Supply Ratio (%) | |
|-----------|---------------------------|-------------|------------|------------------|------------|
| | Precipitation | Groundwater | Soil Water | Precipitation | Soil Water |
| Cropland | −9.24 | −8.44 | −6.49 | 70.82 | 29.18 |
| Grassland | −9.24 | −8.44 | −6.66 | 68.86 | 31.14 |
| Shrubland | −9.24 | −8.44 | −6.52 | 70.53 | 29.47 |
| Woodland | −9.24 | −8.44 | −6.99 | 64.30 | 35.70 |

4. Discussion

4.1. Soil Water Movement and Transformation

In summary, the variation in hydrogen and oxygen isotopic values of shallow soil water is jointly affected by precipitation and evaporation, while the variation in hydrogen and oxygen isotopic values of deep soil water may be affected mostly by infiltration of precipitation and less by evaporation. Precipitation and soil water supply water recharges groundwater. Therefore, the soil water movement mechanism can be analysed by comparing the compositional changes of stable isotopes of precipitation, groundwater, and soil water under different land use types [8].

Precipitation is the only recharge source of soil water in the study area, which falls onto the ground and infiltrates into the soil. One part feeds plant growth and soil evaporation, and the other recharges deep soil and groundwater in the form of matrix and preferential flows. Compared with the Local Meteoric Water Line (LMWL) $\delta\text{D} = 7.82 \delta^{18}\text{O} + 21.51$ ($R^2 = 0.98$, $n = 10$, $p < 0.05$), the slope and intercept of the soil water evaporation line (EL-SW) $\delta\text{D} = 4.68\delta^{18}\text{O} - 24.23$ ($R^2 = 0.86$, $n = 96$, $p < 0.05$) were smaller, and the soil water data points were all distributed below the LMWL (Figure 6), indicating that the soil water was mainly supplied by precipitation and subjected to strong non-equilibrium evaporation, which caused the enrichment of soil D and ^{18}O [37,38]. Most groundwater data points were above the soil water data points. Therefore, groundwater is recharged by a mixture of precipitation and soil water rich in heavy isotopes [7].

Matrix flow and preferential flow are two forms of soil water movement in the soil profile. Matrix flow refers to the movement of soil water driven from top to bottom according to Richard's equation after precipitation infiltration, while preferential flow refers to the movement of some precipitation to recharge the deep soil water or groundwater through soil cracks, vegetation roots, or other channels [3]. Preferential flow can be identified by the high variability of the isotopic signal at a certain soil depth [39,40]. In this study, the stable isotopes (δD and $\delta^{18}\text{O}$) of the soil water showed a gradual trend at 0–200 cm depth (Figure 5), indicating that the soil water moved via matrix flow. The sudden depletion of hydrogen and oxygen isotopes in soil water below 200 cm depth in cropland, grassland, and shrubland indicated the possible presence of a preferential flow, which is consistent with other studies in the Loess Plateau region [41,42].

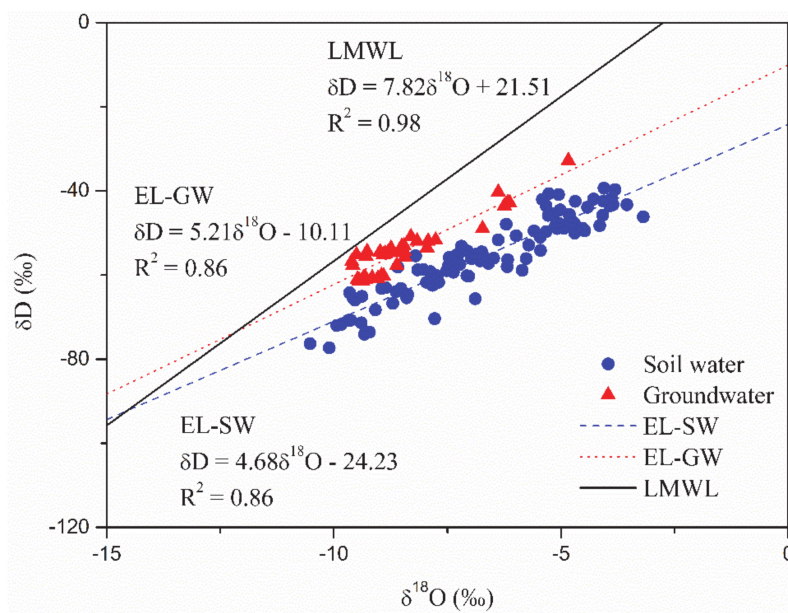


Figure 6. Relationship between δD and $\delta^{18}\text{O}$ of soil water, groundwater, and precipitation. The evaporation line of soil water (EL-SW), evaporation line of groundwater (EL-GW), and local meteoric water line (LMWL) are shown for comparison.

4.2. Influence of Land Use Type on Soil Water Dynamics

The recharge source of soil water under the four land use types in the study area is precipitation. Due to the distance between each soil sampling site is within 1000 m, the precipitation conditions are considered to be the same throughout the area. In addition, vegetation root water absorption cannot change the hydrogen and oxygen isotope compositions [43,44]. Thus, the main reason for the variation in isotopic composition in soil water is the difference in soil evaporation, which is influenced by different vegetation cover. The slope of the soil water evaporation line under four land uses followed this rank order: cropland (4.95) > shrubland (4.85) > grassland (4.75) > woodland (4.48) (Figure 7), indicating that the evaporation and fractionation degree of soil water followed this rank order: cropland < shrubland < grassland < woodland. At the whole study period, the average volumetric soil water content (0–300 cm depth) of cropland ($12.19\% \pm 1.60\%$), shrubland ($9.22\% \pm 1.95\%$), and grassland ($11.38\% \pm 2.29\%$) was higher than that of woodland ($6.56\% \pm 1.79\%$). Thus, the amount of precipitation infiltration was large and fast in agricultural land, shrubland, and grassland, which also proves the existence of soil water preferential flow in these three land use types. Preferential flow has influence on hydrogen and oxygen isotopes in soil profile under different land uses. The degree of evaporation and fractionation of soil water in cropland, shrubland, and grassland was low; thus, less water evaporated, and precipitation was more effective for recharging soil water. In contrast, the degree of evaporation and fractionation of soil water in woodlands was high, the amounts of water received through small precipitation events evaporated rapidly and did not infiltrate in the soil. Only heavy precipitation can recharge soil water.

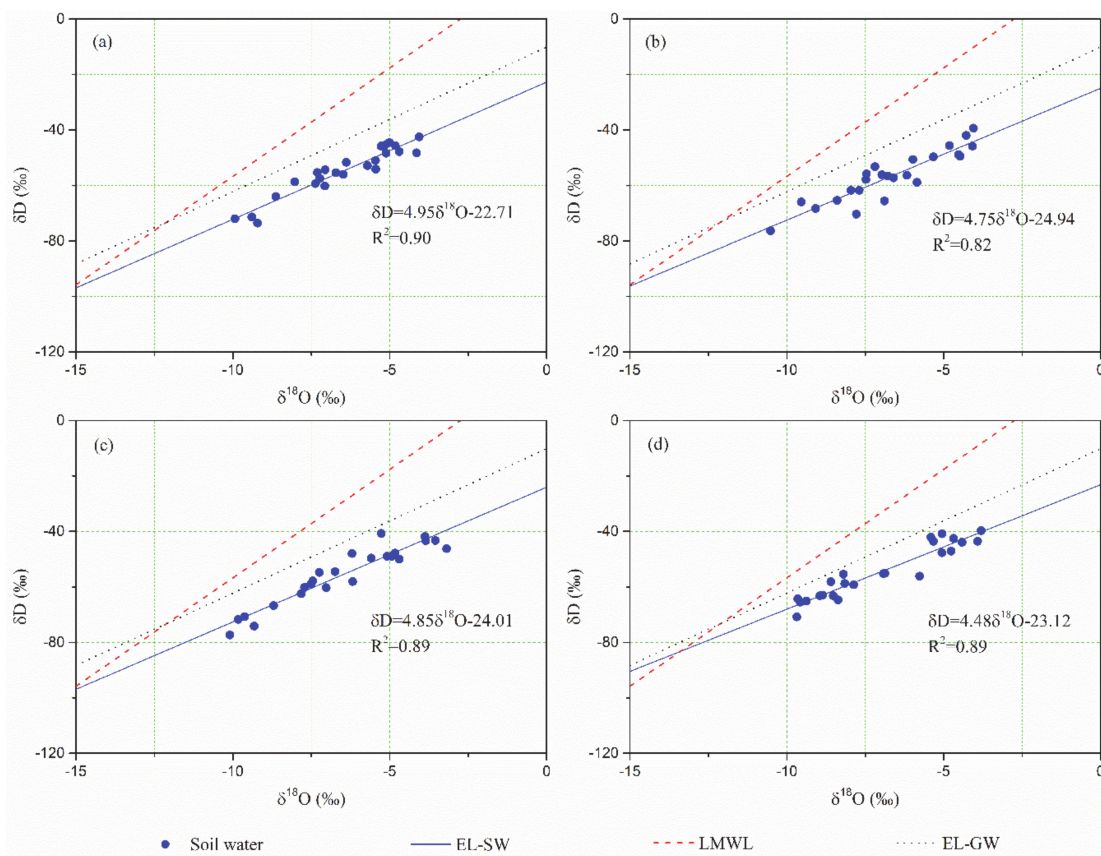


Figure 7. Relationships between δD and $\delta^{18}\text{O}$ of soil water, groundwater and precipitation under different land use types ((a) cropland, (b) grassland, (c) shrubland, (d) woodland).

5. Conclusions

The proportion of groundwater recharge by soil water under different land use types followed this rank order: woodland > grassland > shrubland > cropland. Matrix flow and preferential flow coexisted during infiltration, and the occurrence of preferential flow was related to the land use. The main reason for the variation in isotopic composition in soil water is the difference in soil evaporation, which is influenced by different vegetation cover. The degree of evaporation and fractionation of soil water in cropland, shrubland, and grassland was low; thus, the water was not easily evaporated, and precipitation was more efficient at recharging soil water. However, the degree of evaporation and fractionation of soil water in woodlands was high and small precipitation events were not able to infiltrate and recharge deep soil layers. Moreover, woodland presented a higher surface of soil covered by vegetation, which intercepts some precipitation. Consequently, only heavy precipitation events could recharge soil water in woodlands. These results show that the vegetation cover alters the evaporation rate and the infiltration. The change from cropland, shrubland, and grassland to woodland makes it more difficult for precipitation to recharge deep soil water and groundwater, which hinders sustainable utilisation of groundwater in loess hilly regions.

Author Contributions: Conceptualization, B.Z.; Data curation, L.L.; Funding acquisition, B.Z.; Investigation, K.D.; Project administration, B.Z.; Resources, K.D.; Software, L.L.; Writing—original draft, K.D. and B.Z.; Writing—review & editing, K.D., B.Z. and L.L. All authors have read and agreed to the published version of the manuscript.

Funding: This research was funded by the National Natural Science Foundation of China (Grant No. 41701025), the Postgraduate Student scientific research innovation project of Jiangsu Normal University of China (Grant No. 2019XKT070, No. 2019XKT054).

Institutional Review Board Statement: Not applicable.

Informed Consent Statement: Not applicable.

Data Availability Statement: Data was contained within the article.

Acknowledgments: The authors thank the National Ecosystem Research Network of China and the Institute of Soil and Water Conservation, Chinese Academy of Sciences for meteorological data. We would also like to thank Xuexuan Xu. of the Institute of Soil and Water Conservation for help with analyzing the isotopic samples. We are very grateful to the reviewers and the editors for their constructive comments and thoughtful suggestions.

Conflicts of Interest: The authors declare no conflict of interest.

References

1. Zhao, C.; Jia, X.; Zhu, Y.; Shao, M. Long-term temporal variations of soil water content under different land use types in the Loess Plateau, China. *Catena* **2017**, *158*, 55–62. [[CrossRef](#)]
2. Wei, X.; Si, B.; Biswas, A.; Li, Z. Quantifying dual recharge mechanisms in deep unsaturated zone of Chinese Loess Plateau using stable isotopes. *Geoderma* **2019**, *337*, 773–781.
3. Huang, T.; Ma, B.; Pang, Z.; Li, Z.; Li, Z.; Long, Y. How does precipitation recharge groundwater in loess aquifers? Evidence from multiple environmental tracers. *J. Hydrol.* **2020**, *583*. [[CrossRef](#)]
4. Tan, H.; Liu, Z.; Rao, W.; Wei, H.; Zhang, Y.; Jin, B. Stable isotopes of soil water: Implications for soil water and shallow groundwater recharge in hill and gully regions of the Loess Plateau, China. *Agric. Ecosyst. Environ.* **2017**, *243*, 1–9. [[CrossRef](#)]
5. Jia, X.; Shao, M.; Zhu, Y.; Luo, Y. Soil moisture decline due to afforestation across the Loess Plateau, China. *J. Hydrol.* **2017**, *546*, 113–122. [[CrossRef](#)]
6. Huang, Y.; Chang, Q.; Li, Z. Land use change impacts on the amount and quality of recharge water in the loess tablelands of China. *Sci. Total Environ.* **2018**. [[CrossRef](#)]
7. Zheng, W.; Li, Y.; Gong, Q.; Zhang, H.; Zhao, Z.; Zheng, Z.; Zhai, B.; Wang, Z. Improving yield and water use efficiency of apple trees through intercrop-mulch of crown vetch (*Coronilla varia* L.) combined with different fertilizer treatments in the Loess Plateau. *Span. J. Agric. Res.* **2016**. [[CrossRef](#)]
8. Tan, H.; Liu, Z.; Rao, W.; Jin, B.; Zhang, Y. Understanding recharge in soil-groundwater systems in high loess hills on the Loess Plateau using isotopic data. *Catena* **2017**, *156*, 18–29. [[CrossRef](#)]
9. Gazis, C.; Feng, X. A stable isotope study of soil water: Evidence for mixing and preferential flow paths. *Geoderma* **2004**, *119*, 97–111. [[CrossRef](#)]
10. Xu, X.; Zhao, J.; Zhang, X. Hydrological cycle research by D & ^{18}O tracing in small watershed in the loess hilly region. *Int. Soil Water Conserv. Res.* **2013**, *1*, 75–82.
11. Huang, T.; Yang, S.; Liu, J.; Li, Z. How much information can soil solute profiles reveal about groundwater recharge? *Geosci. J.* **2016**, *20*, 495–502. [[CrossRef](#)]
12. Huang, T.; Pang, Z.; Liu, J.; Yin, L.; Edmunds, W.M. Groundwater recharge in an arid grassland as indicated by soil chloride profile and multiple tracers. *Hydrol. Process.* **2017**, *31*, 1047–1057. [[CrossRef](#)]
13. Zimmermann, U.; Münnich, K.O.; Roether, W.; Kreutz, W.; Schubach, K.; Siegel, O. Tracers determine movement of soil moisture and evapotranspiration. *Science* **1966**, *152*, 346–347. [[CrossRef](#)] [[PubMed](#)]
14. Barnes, C.J.; Allison, G.B. Tracing of water movement in the unsaturated zone using stable isotopes of hydrogen and oxygen. *J. Hydrol.* **1988**, *100*, 143–176. [[CrossRef](#)]
15. Hsieh, J.C.C.; Chadwick, O.A.; Kelly, E.F.; Savin, S.M. Oxygen isotopic composition of soil water: Quantifying evaporation and transpiration. *Geoderma* **1998**, *82*, 269–293. [[CrossRef](#)]
16. Małoszewski, P.; Maciejewski, S.; Stumpp, C.; Stichler, W.; Trimborn, P.; Klotz, D. Modelling of water flow through typical Bavarian soils: 2. Environmental deuterium transport. *Hydrol. Sci. J.* **2006**. [[CrossRef](#)]
17. Sprenger, M.; Erhardt, M.; Riedel, M.; Weiler, M. Historical tracking of nitrate in contrasting vineyards using water isotopes and nitrate depth profiles. *Agric. Ecosyst. Environ.* **2016**, *222*, 185–192. [[CrossRef](#)]
18. Koeniger, P.; Gaj, M.; Beyer, M.; Himmelsbach, T. Review on soil water isotope based groundwater recharge estimations. *Hydrol. Process.* **2016**, *30*, 2817–2834. [[CrossRef](#)]
19. Huang, Y.; Evaristo, J.; Li, Z. Multiple tracers reveal different groundwater recharge mechanisms in deep loess deposits. *Geoderma* **2019**, *353*, 204–212. [[CrossRef](#)]
20. Zheng, W.; Wang, S.; Sprenger, M.; Liu, B.; Gao, J. Response of soil water movement and groundwater recharge to extreme precipitation in a headwater catchment in the North China Plain. *J. Hydrol.* **2019**, *576*, 466–477. [[CrossRef](#)]

21. Ellsworth, P.Z.; Williams, D.G. Hydrogen isotope fractionation during water uptake by woody xerophytes. *Plant Soil* **2007**, *291*, 93–107. [[CrossRef](#)]
22. Gibson, J.J.; Birks, S.J.; Edwards, T.W.D. Global prediction of δA and $\delta^2H - \delta^{18}O$ evaporation slopes for lakes and soil water accounting for seasonality. *Glob. Biogeochem. Cycles* **2008**. [[CrossRef](#)]
23. Dubbert, M.; Piayda, A.; Cuntz, M.; Correia, A.C.; Costa e Silva, F.; Pereira, J.S.; Werner, C. Stable oxygen isotope and flux partitioning demonstrates understory of an oak savanna contributes up to half of ecosystem carbon and water exchange. *Front. Plant Sci.* **2014**. [[CrossRef](#)] [[PubMed](#)]
24. Geris, J.; Tetzlaff, D.; McDonnell, J.J.; Soulsby, C. Spatial and temporal patterns of soil water storage and vegetation water use in humid northern catchments. *Sci. Total Environ.* **2017**, *595*, 486–493. [[CrossRef](#)]
25. Gao, Z.; Lin, Z.; Nin, F.; Luo, J. Soil water dynamics in the active layers under different land-cover types in the permafrost regions of the Qinghai–Tibet Plateau, China. *Geoderma* **2020**, *364*. [[CrossRef](#)]
26. Song, L.; Zhu, J.; Li, M.; Zhang, J.; Wang, K.; Lü, L. Comparison of water-use patterns for non-native and native woody species in a semiarid sandy region of Northeast China based on stable isotopes. *Environ. Exp. Bot.* **2020**, *174*. [[CrossRef](#)]
27. Sun, L.; Yang, L.; Chen, L.; Li, S.; Zhao, F.; Sun, S. Tracing the soil water response to autumn rainfall in different land uses at multi-day timescale in a subtropical zone. *Catena* **2019**, *180*, 355–364. [[CrossRef](#)]
28. Mestas-Valero, R.M.; Miras-Avalos, J.M.; Vidal-Vazquez, E. Estimation of the daily water consumption by maize under Atlantic climatic conditions (A Coruna, NW Spain) using Frequency Domain Reflectometry—A case study. *Nat. Hazards Earth Syst. Sci.* **2012**, *12*, 709–714. [[CrossRef](#)]
29. Yang, L.; Wei, W.; Chen, L.; Chen, W.; Wang, J. Response of temporal variation of soil moisture to vegetation restoration in semi-arid Loess Plateau, China. *Catena* **2014**, *115*, 123–133. [[CrossRef](#)]
30. Chang, E.; Li, P.; Li, Z.; Xiao, L.; Zhao, B.; Su, Y.; Feng, Z. Using water isotopes to analyze water uptake during vegetation succession on abandoned cropland on the Loess Plateau, China. *Catena* **2019**, *181*. [[CrossRef](#)]
31. Wang, J.; Fu, B.; Wang, L.; Lu, N.; Li, J. Water use characteristics of the common tree species in different plantation types in the Loess Plateau of China. *Agric. For. Meteorol.* **2020**, *288*. [[CrossRef](#)]
32. Mirás-Avalos, J.M.; Armesto, M.V.; de Abreu, C.A.; Dias, R.D.; Vazquez, E.V. Temporal Oscillation and Losses of Three Carbon Forms in a Microcatchment of NW Spain. *Commun. Soil Sci. Plant Anal.* **2015**, *46*, 296–308. [[CrossRef](#)]
33. Yeh, H.; Lin, H.; Lee, C.; Hsu, K.; Wu, C. Identifying Seasonal Groundwater Recharge Using Environmental Stable Isotopes. *Water* **2014**, *6*, 2849–2861. [[CrossRef](#)]
34. Wan, H.; Liu, W. An isotope study ($\delta^{18}O$ and δD) of water movements on the Loess Plateau of China in arid and semiarid climates. *Ecol. Engin.* **2016**, *93*, 226–233. [[CrossRef](#)]
35. Zhao, B.; Li, Z.; Li, P.; Cheng, Y.; Gao, B. Effects of ecological construction on the transformation of different water types on Loess Plateau, China. *Ecol. Engin.* **2020**, *144*. [[CrossRef](#)]
36. Sprenger, M.; Leistert, H.; Gimbel, K.; Weiler, M. Illuminating hydrological processes at the soil-vegetation-atmosphere interface with water stable isotopes. *Rev. Geophys.* **2016**, *54*, 674–704. [[CrossRef](#)]
37. Landwehr, J.M.; Coplen, T.B. Spatial, seasonal, and source variability in the stable oxygen and hydrogen isotopic composition of tap waters throughout the USA. *Hydrol. Process.* **2014**, *28*, 5382–5422. [[CrossRef](#)]
38. Chen, T.; Chen, H.; Han, L.; Xing, X.; Fu, Y. Stable Isotopes Characters of Soil Water Movement in Shijiazhuang City. *Environ. Sci.* **2015**, *36*, 3641–3648. (In Chinese)
39. Thomas, E.M.; Lin, H.; Duffy, C.J.; Sullivan, P.L.; Holmes, G.H.; Brantley, S.L.; Jin, L. Spatiotemporal patterns of water stable isotope compositions at the shale hills critical zone observatory: Linkages to subsurface hydrologic processes. *Vadose Zone J.* **2013**. [[CrossRef](#)]
40. Peralta-Tapia, A.; Sponseller, R.A.; Tetzlaff, D.; Soulsby, C.; Laudon, H. Connecting precipitation inputs and soil flow pathways to stream water in contrasting boreal catchments. *Hydrol. Process.* **2015**, *29*, 3546–3555. [[CrossRef](#)]
41. Cheng, L.; Liu, W. Characteristics of stable isotopes in soil water under several typical land use patterns on Loess Tableland. *Chin. J. Appl. Ecol.* **2012**, *23*, 651–658. (In Chinese)
42. Ma, T.; Ke, H.; Li, Z.; Li, P.; Xiao, L.; Zhang, Y.; Tang, S.; Zheng, L.; Su, Y.; Bai, L. Soil water migration characteristics of typical small watershed in rain feed region under individual rainfall events. *J. Soil Water Conserv.* **2018**, *32*, 80–86. (In Chinese)
43. Rong, L.; Chen, X.; Chen, X.; Wang, S.; Du, X. Isotopic analysis of water sources of mountainous plant uptake in a karst plateau of southwest China. *Hydrol. Process.* **2011**, *25*, 3666–3675. [[CrossRef](#)]
44. Zhang, X.; Xiao, Y.; Wan, H.; Deng, Z.; Pan, G.; Xia, J. Using stable hydrogen and oxygen isotopes to study water movement in soil-plant-atmosphere continuum at Poyang Lake wetland, China. *Wetl. Ecol. Manag.* **2017**, *25*, 221–234. [[CrossRef](#)]